



HAL
open science

CuAAC-based assembly and characterization of a ruthenium–copper dyad containing a diimine–dioxime ligand framework

Nicolas Queyriaux, Eugen S. Andreiadis, Stéphane Torelli, Jacques Pécaut, Brad S. Veldkamp, Eric A. Margulies, Michael R. Wasielewski, Murielle Chavarot-Kerlidou, Vincent Artero

► To cite this version:

Nicolas Queyriaux, Eugen S. Andreiadis, Stéphane Torelli, Jacques Pécaut, Brad S. Veldkamp, et al.. CuAAC-based assembly and characterization of a ruthenium–copper dyad containing a diimine–dioxime ligand framework. *Faraday Discussions*, 2017, 198, pp.251-261. 10.1039/C6FD00204H. hal-01534973

HAL Id: hal-01534973

<https://hal.science/hal-01534973>

Submitted on 20 Dec 2023

HAL is a multi-disciplinary open access archive for the deposit and dissemination of scientific research documents, whether they are published or not. The documents may come from teaching and research institutions in France or abroad, or from public or private research centers.

L'archive ouverte pluridisciplinaire **HAL**, est destinée au dépôt et à la diffusion de documents scientifiques de niveau recherche, publiés ou non, émanant des établissements d'enseignement et de recherche français ou étrangers, des laboratoires publics ou privés.

Published in final edited form as:

Faraday Discuss. 2017 June 02; 198: 251–261. doi:10.1039/c6fd00204h.

CuAAC-based assembly and characterization of a ruthenium-copper dyad containing a diimine dioxime ligand framework

Nicolas Queyriaux^a, Eugen S. Andreiadis^a, Stéphane Torelli^a, Jacques Pecaut^b, Brad S. Veldkamp^{c,d}, Eric A. Margulies^{c,d}, Michael R. Wasielewski^{c,d}, Murielle Chavarot-Kerlidou^{a,*}, and Vincent Artero^{a,*}

^aLaboratoire de Chimie et Biologie des Métaux, Univ. Grenoble Alpes, CNRS UMR 5249, CEA, 17 rue des martyrs, F-38054, Grenoble Cedex 9, France

^bUniv. Grenoble Alpes, INAC-SyMMES, F-38000 Grenoble, France; CEA, INAC-SyMMES, Reconnaissance Ionique et Chimie de Coordination, F-38000 Grenoble, France

^cDepartment of Chemistry, Northwestern University, Evanston, Illinois 60208-3113, United States

^dArgonne-Northwestern Solar Energy Research (ANSER) Center, Northwestern University, Evanston, Illinois 60208-3113, United States

Abstract

The design of molecular dyads combining a light-harvesting unit with an electroactive centre is highly demanded in the field of artificial photosynthesis. The versatile Copper-catalyzed Azide-Alkyne Cycloaddition (CuAAC) procedure was employed to assemble a ruthenium tris-diimine unit to an unprecedented azide-substituted copper diimine dioxime moiety. The resulting Ru^{II}Cu^{II} dyad **4** was characterized by electrochemistry, ¹H NMR, EPR, UV-visible absorption, steady-state fluorescence and transient absorption spectroscopies. Photoinduced electron transfer from the ruthenium to the copper centre upon light-activation in presence of a sacrificial electron donor was established thanks to EPR-monitored photolysis experiments, opening interesting perspectives for photocatalytic applications.

Keywords

Copper; ruthenium; CuAAC coupling; light-activated dyad; EPR; photolysis

Introduction

Artificial photosynthetic systems efficiently achieving light-harvesting and solar energy conversion into a chemical potential have been extensively investigated.^{1–7} In the field of solar fuels, their capability to ultimately drive multielectronic redox catalytic processes such as water oxidation, hydrogen evolution or CO₂ reduction is a strong motivation for their development and integration into functional devices.^{8–13} The design and study of novel molecular dyads combining a light-harvesting unit with an electroactive moiety is thus a

* murielle.chavarot-kerlidou@cea.fr; vincent.artero@cea.fr.

major target in the field of artificial photosynthesis. In these multicomponent structures, the establishment of a long-lived charge-separated state through photoinduced intramolecular electron transfer is a crucial requirement for producing functional systems.¹⁴ This is achieved by a judicious choice of the two active units, but also strongly relies on the chemical nature of the covalent bridge. The latter plays a key role in both the charge transport and the charge-separated state lifetime; however, this role is very complex to understand both from a structural and an electronic point of view.^{15–19} There is therefore a great interest in having in hand modular and straightforward synthetic methodologies to synthesize and study structurally-diverse dyad assemblies. In that context, the Copper (I)-catalysed Azide-Alkyne Cycloaddition (CuAAC), one of the best-known examples of “click chemistry”, appears as a unique synthetic tool²⁰: this cycloaddition is efficient under mild conditions, high-yielding and compatible with most organic and metallo-organic functions. For these reasons, CuAAC has been applied to the construction of sophisticated molecular architectures in order to study photoinduced processes.^{21–23} This strategy has been particularly utilized for the functionalization of ruthenium polypyridine photoactive units²⁴ by various organic moieties,^{25–27} nickel^{28, 29} or iron³⁰ complexes and for their attachment onto surfaces.^{31–33} However, to the best of our knowledge, CuAAC has never been employed to assemble a Ru tris-diimine photosensitizer with a copper complex, although copper also displays interesting redox properties. Photoinduced electron transfers in heterodinuclear ruthenium copper complexes have for instance been exploited to develop luminescent probes,^{34–36} molecular switches,³⁷ dye-sensitized solar cells³⁸ and also for the photochemical reduction of nitrite.³⁹ Recently, a RuCu dyad for the photocatalytic oxidation of organic substrates mediated by dioxygen activation has also been reported.⁴⁰ In this contribution, we describe the synthesis and full characterization of the first ruthenium-copper dinuclear complex assembled by CuAAC click chemistry. This dyad consists of a ruthenium polypyridine photoactive unit covalently linked to a copper (II) diimine dioxime complex. EPR-monitored photolysis experiments have been undertaken in combination with detailed photophysical investigations to shed light on the photoinduced electron transfer processes.

Results and discussion

Synthesis

Dyad **4** (Scheme 1) was synthesized by coupling an alkyne-functionalized Ru-trisdiimine light-harvesting moiety **1** with an azide-substituted copper (II) diimine dioxime redox-active unit **2**. The structure of **1**, bearing a functionalized imidazo[4,5-*f*][1,10]phenanthroline ligand, directly stems from supramolecular ruthenium-based assemblies previously studied in our group;^{41, 42} additionally, properties of closely related Ru photosensitizers, displaying the same ligand pattern, are well-studied.^{43, 44} The alkyne function was readily introduced *via* the preparation of the (4-ethynylphenyl)imidazo[4,5-*f*][1,10]phenanthroline ligand and its subsequent metallation with Ru(bpy)₂Cl₂.⁴⁵ Copper (II)-diimine dioxime complexes have been initially reported as biomimetic models for copper-containing metalloproteins.⁴⁶ We previously reported the synthesis of the azido-substituted tetradentate diimine dioxime ligand.^{47, 48} Reaction with copper perchlorate hexahydrate was successfully achieved in 82% yield, as reported for the parent complex [Cu(DO)(DOH)pn(OH₂)](ClO₄).⁴⁹

Deprotonation of one oxime function upon coordination to the divalent metallic salt, characteristic for the diimine dioxime complexes,⁵⁰ yields the monocationic H-bridged Cu^{II} complex **2**. Its molecular structure solved by single crystal X-ray diffraction reveals a square pyramidal geometry for the pentacoordinated copper centre. A displacement of the axially-coordinated water molecule by one oxime oxygen from a neighboring complex is observed and leads to the formation of a polymeric network within the lattice (Fig. S1), as previously observed for [Cu(DO)(DOH)pn(OH₂)](ClO₄).⁵⁰

Classical CuAAC procedures, recently applied to related ruthenium tris-diimine complexes, ^{26, 51} rely on the combination of copper (II) sulfate with sodium ascorbate to generate *in-situ* the catalytically-active copper (I) species. The reactivity of **1** under these conditions was first tested with a commercially-available benzyl azide as model partner. In our hands, the procedure was optimized by employing a homogeneous ternary solvent mixture (CH₂Cl₂/MeOH/H₂O) and benzyltriazole-functionalized complex **3** was isolated in 65 % yield after purification (see S.I.). These new conditions were then applied for the coupling of **1** with azide-functionalized complex **2**. After purification by chromatography on silica gel, dyad **4** was isolated as a dark-orange powder in 55 % yield.

¹H NMR spectroscopy

¹H NMR spectra have been recorded in CD₃CN for the three Ru complexes. Spectra of compounds **3** (Fig. S2) and **4** (Fig. S3) are characterized by the complete disappearance of the alkyne proton signal, observed at 3.56 ppm for **1**. In addition, spectrum of **3** displays two new signals, a singlet at 5.63 ppm for the benzylic CH₂ protons (Fig. S2) and a singlet at 8.24 ppm attributed to the aromatic proton on the newly-formed 1,2,3-triazole unit (Fig. 1, red trace, arrow).

The presence of the paramagnetic Cu^{II} centre in **4** however prevents the detection of the CH₃, CH₂ and CH groups from the diimine dioxime ligand in the aliphatic region of the spectrum. This is also true for the triazolyl proton, expected to appear as a singlet in the aromatic region, by comparison with **3**, and for the phenylene protons *ortho* to the triazole ring (7.67 ppm in **1** and 8.06 ppm in **3**). In addition, the signal of the two other phenylene protons appears as the large signal in the baseline around 8.4 ppm (Fig. 1, green trace, dashed arrow) and a light broadening is observed at 9.04 and 7.80 ppm for the H^{4/7} and H^{3/8} protons of the phenanthroline ring respectively (Fig. 1, green trace, dashed arrows), more distant from the Cu^{II} centre.

Electrochemistry

The electrochemical properties of dyad **4** and of the two precursors **1** and **2** were investigated by cyclic voltammetry. Data are summarized in Table 1 and the voltammograms are displayed in Fig. S5. Complexes **1** and **4** exhibit redox features characteristic for ruthenium tris-diimine complexes, with a reversible Ru^{III}/Ru^{II} process at +0.88 V and +0.93 V *vs* Fc⁺⁰, respectively, thus only slightly affected by the coupling. Three reduction processes take place between -1.7 and -2.4 V *vs* Fc⁺⁰, corresponding to the reduction of the three diimine ligands in the Ru^{II} coordination sphere (the first one more likely occurring on the π-acceptor imidazolophenanthroline ligand). An additional cathodic wave is observed at

– 0.95 V (E_{pa}) for **4**, attributed to the Cu^{II}/Cu^I process by comparison with the azide precursor **2** (Fig. S5). Loss of reversibility is observed for this process in **4**, indicative for a fast chemical reaction or structural rearrangement that can be partially outrun at higher scan rates ($10\text{ V}\cdot\text{s}^{-1}$). Overall, redox properties of dyad **4** compare well with those from the independent Ru and Cu subunits **1** and **2**, thus underlining that the two metallic centres are not coupled in the electronic ground state.

UV-vis absorption spectroscopy

Absorption spectra were recorded for **1**, **2** and **4** at a concentration of $2 \times 10^{-5}\text{ M}$ in acetonitrile. Compounds **1** and **4** display a broad absorption band in the visible region, centred at 455 nm with a shoulder at 430 nm, characteristic of the Metal-to-Ligand-Charge-Transfer (1MLCT) transition of the ruthenium tris-diimine moiety. A slight contribution from the absorption of the copper diimine-dioxime moiety can be observed in the UV region for **4**, by comparison with **2**. The spin-forbidden d–d transition of the copper complex can be observed at 480 nm for this family of complexes,⁵² with a very low molar absorptivity ($\approx 200\text{ L}\cdot\text{Mol}^{-1}\cdot\text{cm}^{-1}$, Fig. S6). Overall, the absorption spectrum of dyad **4** can be simply described as the superimposition of its individual components **1** and **2** (dotted line in Fig. 2) with a slight contribution at 326 nm tentatively attributed to the newly formed triazole ring; this observation is again in good agreement with the absence of significant ground state electronic interaction between the two electroactive moieties.

The Cu^I spectroscopic features have been determined by spectroelectrochemical reduction on the parent complex $[Cu(DO)(DOH)pn(OH_2)](ClO_4)$. Disappearance of the weak Cu^{II} signal around 480 nm concomitantly with the appearance of a new signal at 665 nm attributed to the reduced Cu^I complex^{49, 53} were observed during the course of an electrolysis experiment at an applied potential of $-0,70\text{ V vs Ag/AgCl}$ (Figure S6).

Steady-state fluorescence spectroscopy

Emission spectra were recorded for isoabsorptive solutions of **1** and **4** in acetonitrile. Typical emission signals for ruthenium tris-diimine photosensitizers are obtained, without any shift of the maximum emission wavelength ($\lambda_{em} = 604\text{ nm}$). Dyad **4** is, on the other hand, characterized by a 50 % quenching of the emission of the ruthenium centre, compared to **1**. Two different photoinduced processes could account for this quenching: either energy transfer or intramolecular electron transfer from the ruthenium excited state (*Ru) to the copper (II) moiety. Although the d-d band of **2** partially overlaps the emission signal of the ruthenium centre, energy transfer is very unlikely to occur: the very low absorption coefficient of this metal-centered transition indeed strongly disfavors the Förster mechanism and the Dexter mechanism is spin forbidden. According to (i) the $Cu^{II/I}$ reduction potential (Table 1), (ii) the $Ru^{III/II}$ oxidation potential (Table 1) and (iii) the *Ru excited state energy E_{00} (2.12 eV),^{54, 55} the oxidative quenching of *Ru by photoinduced electron transfer to the copper (II) moiety is estimated to be feasible with a relatively low thermodynamic driving force ($G_{ET} = -0.24\text{ eV}$).⁵⁶ The ability of 1,2,3-triazole bridges to mediate charge transport has been particularly evaluated with porphyrin-based dyads and triads, albeit with some differences in their efficiencies.^{57–60} When considering Ru tris-diimine-based

assemblies, however, the few reported examples by Aukauloo and co-workers gave evidence for the efficiency of such triazole-based bridging units.^{25, 26, 28}

EPR-monitored photolysis experiment

EPR spectroscopy is the technique of choice to bring any metal redox state modification to light. It has been previously employed in the literature to characterize light-induced redox processes such as oxidation of a Ni^{II} centre²⁹ or reduction of a Cu^{II} centre⁴⁰ in ruthenium-based dyads, under photolysis conditions. Reductive photolysis experiments are typically performed in the presence of a large excess of a sacrificial electron donor, such as triethylamine (TEA); the latter rapidly reacts with the oxidized photosensitizer to regenerate Ru^{II}, thus avoiding charge recombination and leading to accumulation of the targeted reduced species. To probe the occurrence of a photoinduced electron transfer with **4**, a photolysis experiment was monitored using EPR. The spectrum of **4** (Fig. S7) is characteristic for a mononuclear copper centre in axial symmetry ($g_{\parallel} > g_{\perp}$) with a hyperfine coupling of 20.3 mT, similar to the azide-precursor **2** (Fig. S7) and to the literature.⁵³ Thus, no significant modification of the copper diimine dioxime geometry occurs, either upon coupling with **1** (Fig. S7), or in presence of 200 equivalents of TEA (Fig. 3; $t = 0$ min). However, the EPR signal decreases upon visible light irradiation and is almost completely silent after 30 minutes (Fig. 3).

Additional experiments have showed that light and TEA are both required for the disappearance of signal (Fig. S8 and S9). The complete disappearance of the EPR signal associated with the Cu^{II} centre in **4** thus clearly establishes that photoinduced electron transfer occurs upon light-activation of dyad **4** in presence of a sacrificial electron donor, leading to the formation of the EPR-silent reduced Cu^I species. Two mechanisms can operate under these photolysis conditions: (i) the oxidative quenching pathway, previously discussed in the “steady-state fluorescence spectroscopy” section, which forms a Ru^{III}Cu^I intermediate before regeneration of the Ru^{II} centre by the sacrificial electron donor TEA; (ii) the reductive quenching pathway, where *Ru is first quenched by TEA, yielding a Ru^ICu^{II} species, that ultimately produced Ru^{II}Cu^I. The oxidative quenching process was unambiguously established, on the basis of time-resolved spectroscopic studies, for two dyads we previously studied: a ruthenium-cobalt one, also relying on an imidazo[4,5-f][1,10]phenanthroline bridging ligand,⁴¹ and more recently a ruthenium-copper assembly.⁴⁰ Moreover, previous reports have established that quenching of *[Ru(bpy)₃]²⁺ and related Ru-based photosensitizers by aliphatic amines (TEA, TEOA) was not efficient, even at high molar concentrations of the quencher,^{61–63} supporting the fact that a reductive quenching process is quite unlikely to occur in our system.

Transient absorption spectroscopy

Femtosecond and nanosecond transient absorption studies have been carried out in order to obtain the kinetics for the photoinduced intramolecular processes. The femtosecond transient absorption spectra of complexes **1**, **3** and **4** are similar (Fig. S10-S12). Photoexcitation of the ruthenium centre with 414 nm light generates *Ru, which exhibits broad absorption at wavelengths longer than 500 nm together with ground state bleach near 450 nm. After the initial rise of these features, the spectra exhibit little change as the pump to probe delay is

increased step-wise to 5.4 ns. Specifically, no new signal arises around 665 nm for **4**, which would be characteristic for Cu^I.

In the nanosecond transient absorption experiments (Fig. S13-S14), stimulated emission from the *Ru excited state is observed between 565 nm and 725 nm, in addition to ground state bleaching and excited state absorption. For **3**, the excited state lifetime is 1.07 ± 0.05 μ s, based on the kinetics at 460 nm, 540 nm, 620 nm and 800 nm. For dyad **4**, a faster excited state decay is observed, with a lifetime of 0.38 ± 0.01 μ s. However, the formation of an intermediate state with a longer lifetime is very unlikely as the ground state bleach, the excited state absorbance and the emission all decay at nearly equal rates. The origin of this shortened lifetime is not clear. The presence of the paramagnetic Cu^{II} species may enhance the rate of intersystem crossing from the Ru-based ³*MLCT state back to the ground state. Alternatively, electron transfer from the *Ru excited state to the Cu(II) centre followed by *faster* charge recombination can also explain the increased decay rate without observation of an intermediate species. Similar behavior has been previously reported for another dyad featuring a triazole bridge, where charge separation was slower than charge recombination, thus preventing accumulation of the charge separated state to any appreciable extent.^{19, 59}

Conclusion

There is an important need for developing modular and efficient methodologies to assemble molecular photosensitizers and catalysts into covalent photocatalytic systems. Diimine-dioxime cobalt complexes are well-known as hydrogen-forming electrocatalysts.⁶⁴ As a first step towards the formation of a cobalt-based photocatalytic dyad, we exploited the versatility of the CuAAC methodology to covalently couple a ruthenium tris-diimine photosensitizer with a copper diimine dioxime redox-active unit. Dyad **4** is the first example of a dinuclear Ru^{II}Cu^{II} complex assembled through click chemistry. It has been characterized extensively by ¹H NMR, cyclic voltammetry, UV-vis absorption, fluorescence and EPR spectroscopies. A 50 % quenching of the ruthenium-centred fluorescence is observed in dyad **4**, although specific signatures and kinetics related to the intramolecular photo-induced electron transfer could not be obtained from ultrafast spectroscopy experiments, possibly due to a fast recombination process. Under continuous photolysis conditions, the sacrificial electron donor, however, regenerates the ruthenium ground state faster than charge recombination and allows for photoaccumulation of the Ru^{II}Cu^I compound. This result opens interesting perspectives for the application of dyad **4** and derivatives in the field of photocatalysis.

Typical procedure for the CuAAC coupling

4. In a round bottom flask, **1** (80 mg, 0,08 mmol) and **3** (70 mg, 0.16 mmol) were dissolved in a homogeneous solvent mixture of MeOH, CH₂Cl₂ and H₂O (3:3:1; 15 mL). The solution was degassed with argon before the addition of sodium ascorbate (80 mg, 0.39 mmol) and copper sulfate (8 mg, 0.03 mmol). The reaction mixture was stirred at 50°C under argon in the dark over the weekend. The organic solvents were evaporated and the desired compound was precipitated by dropwise addition of a saturated KPF₆ aqueous solution. The orange precipitate was filtered, washed with water and dried under vacuum. The crude product was purified by column chromatography on silica gel (MeCN/0.4M aqueous KNO₃, 80:20). The

fractions were concentrated and the product precipitated by dropwise addition of a saturated KPF_6 aqueous solution. The precipitate was filtered, washed with water and dried under vacuum to give 65 mg (55 % yield) of **4** as a dark orange powder.

^1H NMR (400 MHz, CD_3CN) δ 9.04 (sbr, 2H), 8.53 (dd, $J = 16.1, 8.1$ Hz, 4H), 8.44 (sbr, 4H), 8.11 (dd, $J = 7.8$ Hz, 2H), 8.01 (dd, $J = 17.2, 6.3$ Hz, 4H), 7.87 (d, $J = 5.2$ Hz, 2H), 7.80 (sbr, 2H), 7.61 (d, $J = 5.3$ Hz, 2H), 7.46 (dd, $J = 6.4$ Hz, 2H), 7.23 (dd, $J = 6.3$ Hz, 2H). MS (ESI+) m/z 1368 $[\text{M} - \text{H}_2\text{O} - \text{PF}_6]^+$, m/z 611 $[\text{M} - \text{H}_2\text{O} - 2\text{PF}_6]^{2+}$, m/z 538 $[\text{M} - \text{H}_2\text{O} - 3\text{PF}_6 - \text{H}]^{2+}$, m/z 359 $[\text{M} - \text{H}_2\text{O} - 3\text{PF}_6]^{3+}$. HRMS (ESI+) calculated for $\text{C}_{52}\text{H}_{46}\text{CuN}_{15}\text{O}_2\text{Ru}$ 359.0764; found 359.0767. Elemental analysis (%), calculated for $\text{C}_{52}\text{H}_{48}\text{CuF}_{18}\text{N}_{15}\text{O}_3\text{P}_3\text{Ru} + 0.8 \text{KPF}_6$: C 37.93, H 2.94, N 12.76; found: C 38.27, H 3.20, N 12.36.

Supplementary Material

Refer to Web version on PubMed Central for supplementary material.

Acknowledgements

This work was supported by the Life Science Division of CEA (2011 DSV-Energy program), the COST Action CM1202 PERSPECT-H₂O, the French National Research Agency (Labex program, ARCANÉ, ANR-11-LABX-0003-01) and the European Research Council under the European Union's Seventh Framework Program (FP/2007-2013)/ERC Grant Agreement n.306398. Work at Northwestern University was supported by the Argonne-Northwestern Solar Energy Research (ANSER) Center, an Energy Frontier Research Center funded by the U.S. Department of Energy (DOE), Office of Science, Office of Basic Energy Sciences, under award number DE-SC0001059. Colette Lebrun and Daniel Imbert (CEA, INAC- SCIB) are acknowledged for the ESI-MS and the fluorescence measurements, respectively.

References

1. Wasielewski MR. *Chem Rev.* 1992; 92:435–461.
2. Harriman A, Sauvage JP. *Chem Soc Rev.* 1996; 25:41–&.
3. Gust D, Moore TA, Moore AL. *Acc Chem Res.* 2001; 34:40–48. [PubMed: 11170355]
4. Fukuzumi S. *Phys Chem Chem Phys.* 2008; 10:2283–2297. [PubMed: 18414719]
5. Flamigni L, Collin JP, Sauvage JP. *Acc Chem Res.* 2008; 41:857–871. [PubMed: 18543956]
6. Aratani N, Kim D, Osuka A. *Acc Chem Res.* 2009; 42:1922–1934. [PubMed: 19842697]
7. Wasielewski MR. *Acc Chem Res.* 2009; 42:1910–1921. [PubMed: 19803479]
8. Andreiadis ES, Chavarot-Kerlidou M, Fontecave M, Artero V. *Photochem Photobiol.* 2011; 87:946–964. [PubMed: 21740444]
9. Berardi S, Drouet S, Francas L, Gimbert-Surinach C, Guttentag M, Richmond C, Stoll T, Llobet A. *Chem Soc Rev.* 2014; 43:7501–7519. [PubMed: 24473472]
10. Herrero C, Quaranta A, Leibl W, Rutherford AW, Aukauloo A. *Energy Environ Sci.* 2011; 4:2353–2365.
11. Morris AJ, Meyer GJ, Fujita E. *Acc Chem Res.* 2009; 42:1983–1994. [PubMed: 19928829]
12. Gust D, Moore TA, Moore AL. *Acc Chem Res.* 2009; 42:1890–1898. [PubMed: 19902921]
13. Song W, Chen Z, Brennaman MK, Concepcion JJ, Patrocinio AOT, Iha NYM, Meyer TJ. *Pure Appl Chem.* 2011; 83:749–768.
14. Wenger OS. *Coord Chem Rev.* 2009; 253:1439–1457.
15. Hanss D, Walther ME, Wenger OS. *Coord Chem Rev.* 2010; 254:2584–2592.
16. Wenger OS. *Acc Chem Res.* 2011; 44:25–35. [PubMed: 20945886]
17. Schulz M, Karnahl M, Schwalbe M, Vos JG. *Coord Chem Rev.* 2012; 256:1682–1705.

18. Arrigo A, Santoro A, Indelli MT, Natali M, Scandola F, Campagna S. *Phys Chem Chem Phys*. 2014; 16:818–826. [PubMed: 24287945]
19. Natali M, Campagna S, Scandola F. *Chem Soc Rev*. 2014; 43:4005–4018. [PubMed: 24604096]
20. Kolb HC, Finn MG, Sharpless KB. *Angew Chem Int Ed*. 2001; 40:2004–2021.
21. Ladomenou K, Nikolaou V, Charalambidis G, Coutsolelos AG. *Coord Chem Rev*. 2016; 306(Part 1):1–42.
22. Nierengarten I, Nierengarten J-F. *Chem Rec*. 2015; 15:31–51. [PubMed: 25392909]
23. Odobel F, Séverac M, Pellegrin Y, Blart E, Fosse C, Cannizzo C, Mayer CR, Elliott KJ, Harriman A. *Chemistry – A European Journal*. 2009; 15:3130–3138.
24. Zabarska N, Stumper C, Rau S. *Dalton Trans*. 2016; 45:2338–2351. [PubMed: 26758682]
25. Baron A, Herrero C, Quaranta A, Charlot M-F, Leibl W, Vauzeilles B, Aukauloo A. *Chem Commun*. 2011; 47:11011–11013.
26. Baron A, Herrero C, Quaranta A, Charlot M-F, Leibl W, Vauzeilles B, Aukauloo A. *Inorg Chem*. 2012; 51:5985–5987. [PubMed: 22590981]
27. Sheth S, Baron A, Herrero C, Vauzeilles B, Aukauloo A, Leibl W. *Photochem Photobiol Sci*. 2013; 12:1074–1078. [PubMed: 23558787]
28. Herrero C, Batchelor L, Baron A, El Ghachtouli S, Sheth S, Guillot R, Vauzeilles B, Sircoglou M, Mallah T, Leibl W, Aukauloo A. *Eur J Inorg Chem*. 2013; 2013:494–499.
29. Herrero C, Quaranta A, El Ghachtouli S, Vauzeilles B, Leibl W, Aukauloo A. *Phys Chem Chem Phys*. 2014; 16:12067–12072. [PubMed: 24600692]
30. Herrero C, Quaranta A, Sircoglou M, Senechal-David K, Baron A, Marin IM, Buron C, Baltaze J-P, Leibl W, Aukauloo A, Banse F. *Chemical Science*. 2015; 6:2323–2327.
31. Benson MC, Ruther RE, Gerken JB, Rigsby ML, Bishop LM, Tan Y, Stahl SS, Hamers RJ. *ACS Applied Materials & Interfaces*. 2011; 3:3110–3119. [PubMed: 21766849]
32. Ruther RE, Rigsby ML, Gerken JB, Hogendoorn SR, Landis EC, Stahl SS, Hamers RJ. *J Am Chem Soc*. 2011; 133:5692–5694. [PubMed: 21438578]
33. Gerken JB, Rigsby ML, Ruther RE, Pérez-Rodríguez RJ, Guzei IA, Hamers RJ, Stahl SS. *Inorg Chem*. 2013; 52:2796–2798. [PubMed: 23458735]
34. Comba P, Krämer R, Mokhir A, Naing K, Schatz E. *Eur J Inorg Chem*. 2006; 2006:4442–4448.
35. Zhang R, Yu X, Yin Y, Ye Z, Wang G, Yuan J. *Anal Chim Acta*. 2011; 691:83–88. [PubMed: 21458635]
36. Gei, Alsfasser R. *Dalton Trans*. 2003; :612–618. DOI: 10.1039/B209930F
37. Ishizuka T, Tobita K, Yano Y, Shiota Y, Yoshizawa K, Fukuzumi S, Kojima T. *J Am Chem Soc*. 2011; 133:18570–18573. [PubMed: 22017339]
38. McCall KL, Jennings JR, Wang H, Morandeira A, Peter LM, Durrant JR, Yellowlees LJ, Robertson N. *Eur J Inorg Chem*. 2011; 2011:589–596.
39. Isoda N, Torii Y, Okada T, Misoo M, Yokoyama H, Ikeda N, Nojiri M, Suzuki S, Yamaguchi K. *Dalton Trans*. 2009; :10175–10177. DOI: 10.1039/B907484H [PubMed: 19921050]
40. Iali W, Lanoe P-H, Torelli S, Jouvenot D, Loiseau F, Lebrun C, Hamelin O, Ménage S. *Angew Chem Int Ed*. 2015; 54:8415–8419.
41. Fihri A, Artero V, Razavet M, Baffert C, Leibl W, Fontecave M. *Angew Chem Int Ed*. 2008; 47:564–567.
42. Fihri A, Artero V, Pereira A, Fontecave M. *Dalton Trans*. 2008:5567–5569. [PubMed: 18854893]
43. Quaranta A, Lachaud F, Herrero C, Guillot R, Charlot M-F, Leibl W, Aukauloo A. *Chemistry – A European Journal*. 2007; 13:8201–8211.
44. Reichardt C, Sainuddin T, Wächtler M, Monro S, Kupfer S, Guthmuller J, Gräfe S, McFarland S, Dietzek B. *J Phys Chem A*. 2016; 120:6379–6388. [PubMed: 27459188]
45. Ramachandra S, Schuermann KC, Edafe F, Belser P, Nijhuis CA, Reus WF, Whitesides GM, De Cola L. *Inorg Chem*. 2010; 50:1581–1591. [PubMed: 21194229]
46. Gagne RR, Allison JL, Gall RS, Koval CA. *J Am Chem Soc*. 1977; 99:7170–7178. [PubMed: 915148]

47. Jacques, PA., Artero, V., Fontecave, M., Leyris, A., Matheron, M. French patent application EN10 53019 deposited in France. International PCT extension; USA, Japan, China, India: 2010 Apr 20. deposited April 20 2011
48. Andreiadis ES, Jacques P-A, Tran PD, Leyris A, Chavarot-Kerlidou M, Jousset B, Matheron M, Pécaut J, Palacin S, Fontecave M, Artero V. *Nat Chem.* 2013; 5:48–53. [PubMed: 23247177]
49. Gagne RR. *J Am Chem Soc.* 1976; 98:6709–6710. [PubMed: 972225]
50. Bertrand JA, Smith JH, VanDerveer DG. *Inorg Chem.* 1977; 16:1484–1488.
51. Kroll A, Monczak K, Sorsche D, Rau S. *Eur J Inorg Chem.* 2014; 2014:3462–3466.
52. Protasiewicz GM, Nunes FS. *Spectrochim Acta Part A.* 2006; 65:549–552.
53. Addison AW, Carpenter M, Lau LKM, Wicholas M. *Inorg Chem.* 1978; 17:1545–1552.
54. Juris A, Balzani V, Barigelli F, Campagna S, Belser P, von Zelewsky A. *Coord Chem Rev.* 1988; 84:85–277.
55. Campagna S, Puntoriero F, Nastasi F, Bergamini G, Balzani V. *Top Curr Chem.* 2007; 280:117–214.
56. The Gibbs energy of formation of the CuI species by electron transfer from Ru* to CuII was calculated using the equation: $DG1^\circ = E(\text{RuIII}/\text{RuII}) - E00 - E(\text{CuII}/\text{CuI})$.
57. Harriman A, Elliott KJ, Alamiry MAH, Pleux LL, Séverac M, Pellegrin Y, Blart E, Fosse C, Cannizzo C, Mayer CR, Odobel F. *J Phys Chem C.* 2009; 113:5834–5842.
58. de Miguel G, Wielopolski M, Schuster DI, Fazio MA, Lee OP, Haley CK, Ortiz AL, Echegoyen L, Clark T, Guldi DM. *J Am Chem Soc.* 2011; 133:13036–13054. [PubMed: 21702513]
59. Natali M, Ravaglia M, Scandola F, Boixel J, Pellegrin Y, Blart E, Odobel F. *J Phys Chem C.* 2013; 117:19334–19345.
60. Nikolaou V, Karikis K, Farre Y, Charalambidis G, Odobel F, Coutsolelos AG. *Dalton Trans.* 2015; 44:13473–13479. [PubMed: 26160267]
61. Krishnan CV, Brunschwig BS, Creutz C, Sutin N. *J Am Chem Soc.* 1985; 107:2005–2015.
62. Goldsmith JI, Hudson WR, Lowry MS, Anderson TH, Bernhard S. *J Am Chem Soc.* 2005; 127:7502–7510. [PubMed: 15898800]
63. Zhang P, Wang M, Na Y, Li X, Jiang Y, Sun L. *Dalton Trans.* 2010; 39:1204–1206. [PubMed: 20104346]
64. Kaeffer N, Chavarot-Kerlidou M, Artero V. *Acc Chem Res.* 2015; 48:1286–1295. [PubMed: 25941953]

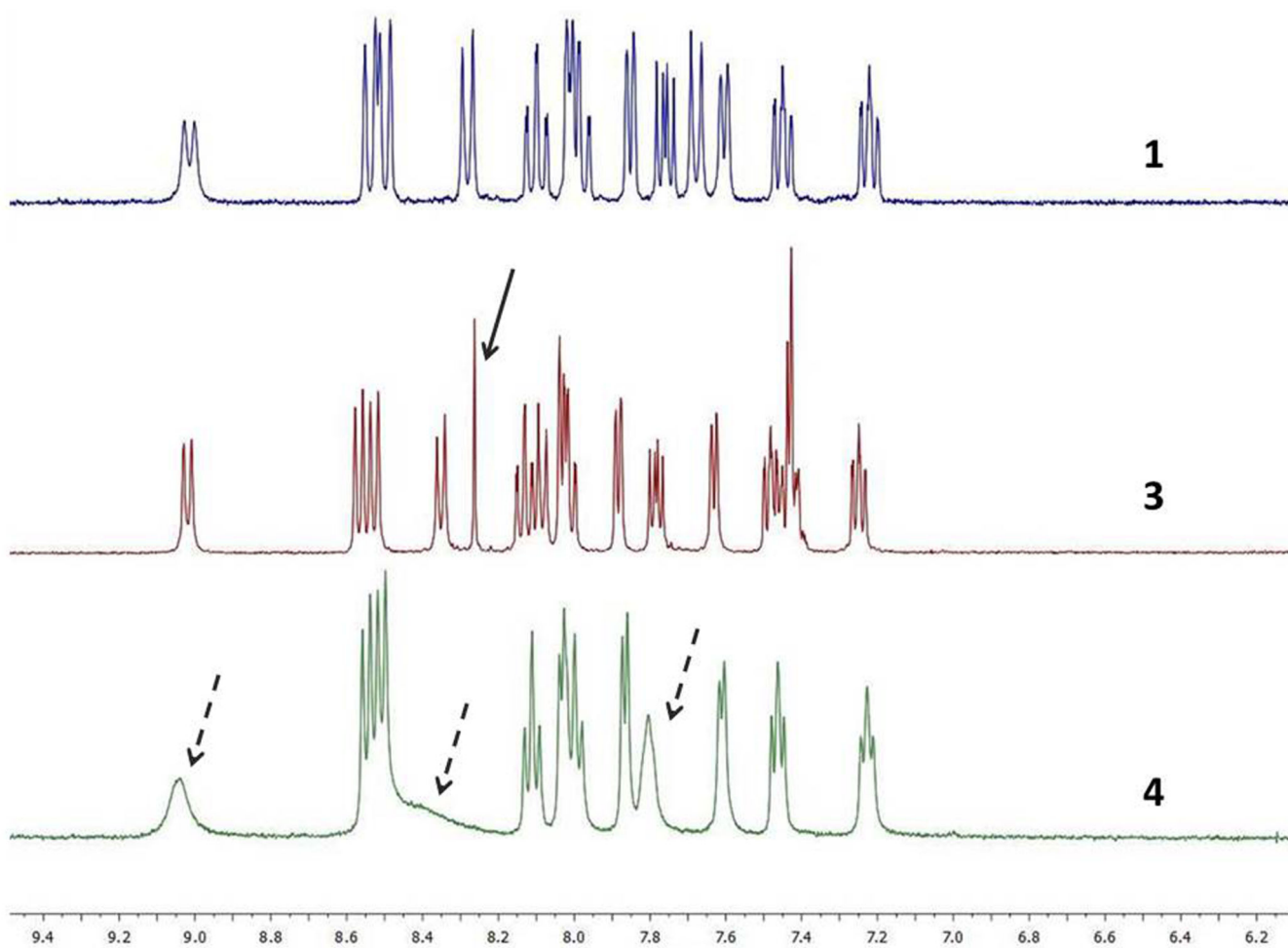


Figure 1.
Aromatic region of the ^1H NMR spectra recorded for **1**, **3** and **4** in CD_3CN .

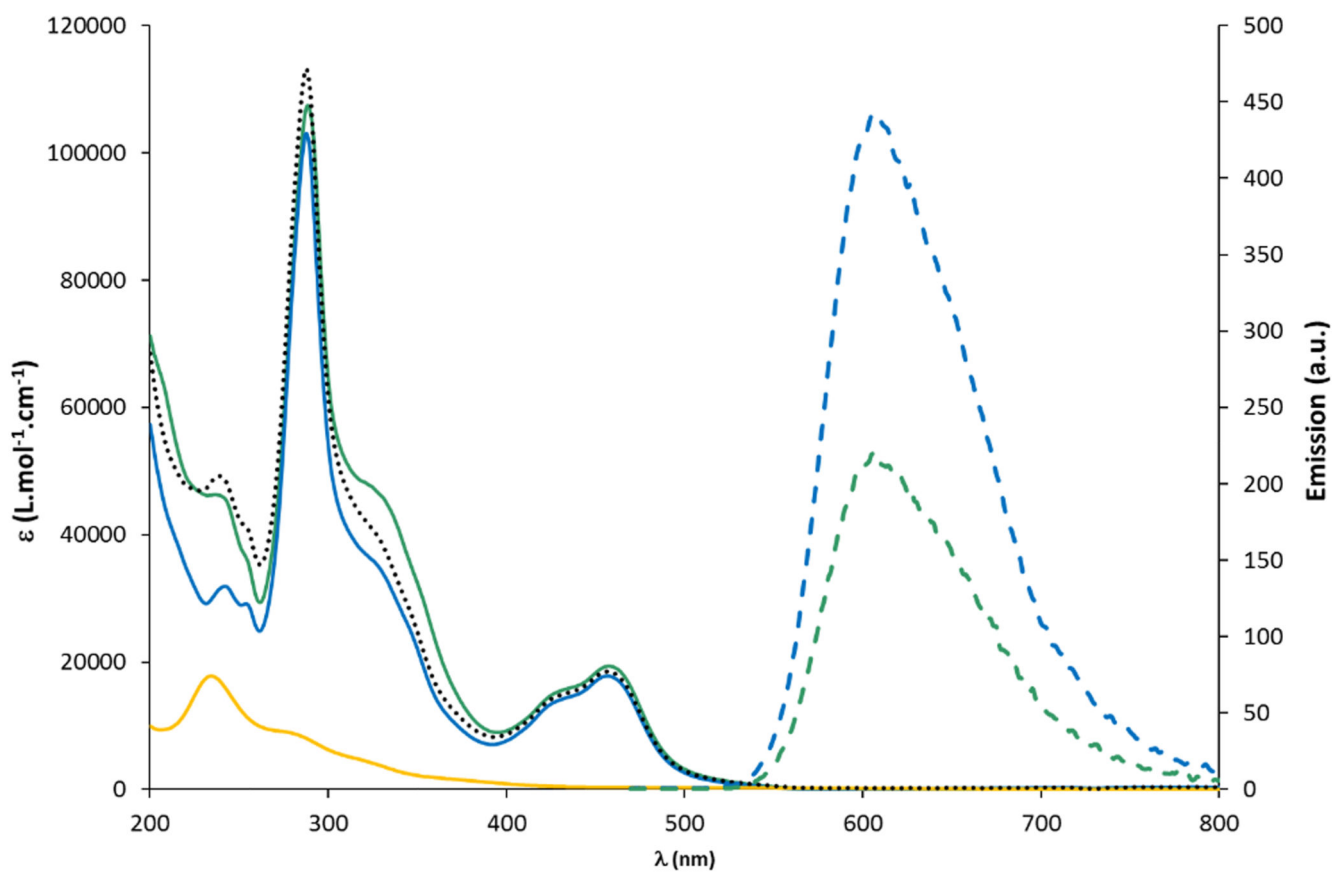


Figure 2. Absorption spectra of **1** (blue), **2** (orange) and **4** (green) recorded at 2.10^{-5} M in acetonitrile and room temperature emission spectra ($\lambda_{\text{exc}} = 450$ nm) of isoabsorptive solutions of **1** (dashed blue) and **4** (dashed green) in acetonitrile.

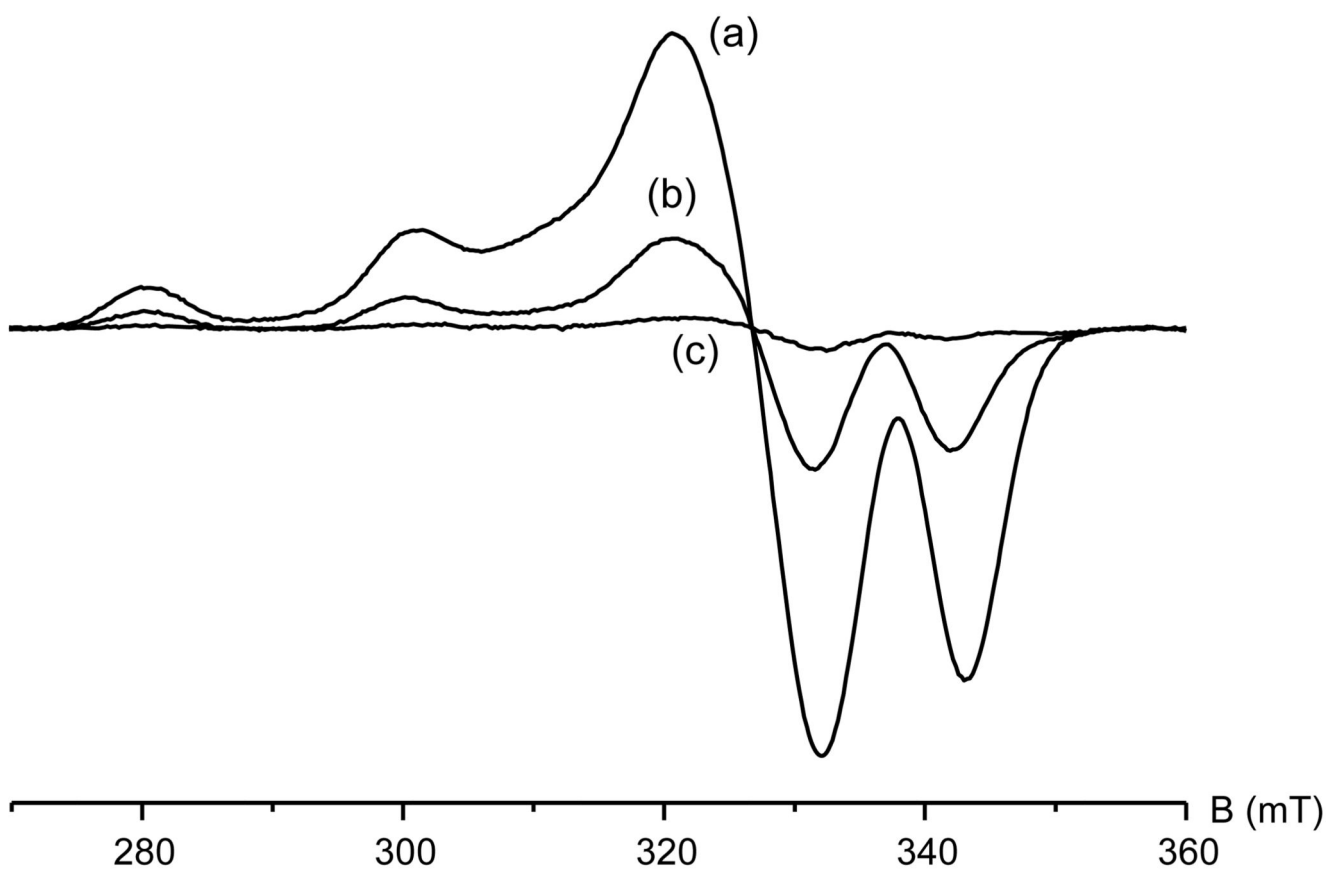
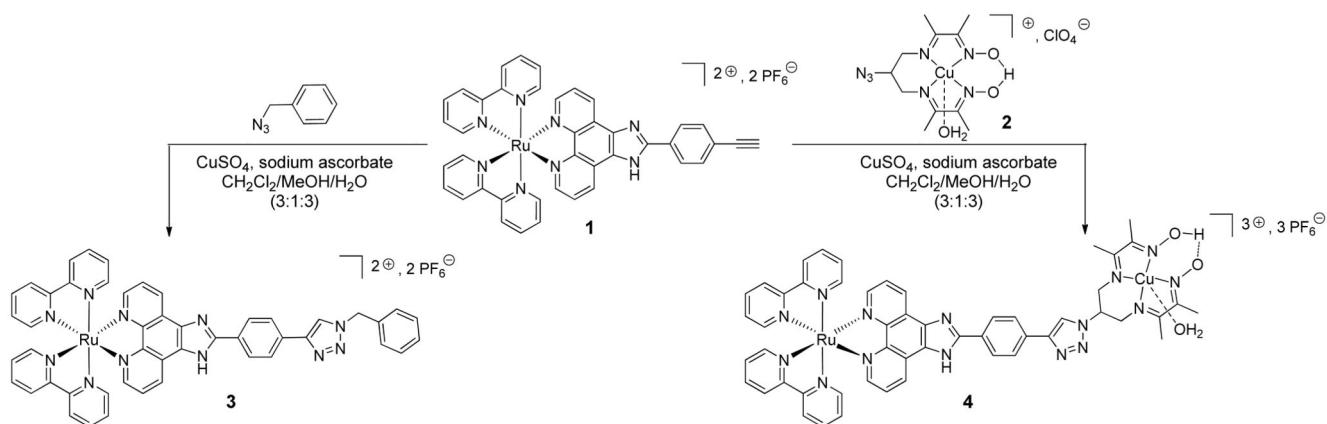


Figure 3. X band EPR spectra of complex **4** (1 mM) recorded at 42 K before (a) and after 15 min (b) and 30 min (c) irradiation time in CH_3CN in presence of TEA (200 molar eq.). Microwave frequency: 9.4 GHz; modulation amplitude: 12 G; modulation frequency: 100 kHz; microwave power: 0.5 mW).

**Scheme 1.**

CuAAC coupling between alkyne-substituted ruthenium tris-diimine complex **1** and azide-substituted copper (II) diimine dioxime complex **2**, yielding RuCu dyad **4**.

Table 1

Redox properties^a of compounds **1**, **2** and **4** determined by cyclic voltammetry at 100 mV.s⁻¹ in a CH₃CN solution of *n*-Bu₄NBF₄ (0.1 mol.L⁻¹).

	1	2	4
Ru ^{III} /Ru ^{II} ^b	+0.88 V	—	+0.93 V
Cu ^{III} /Cu ^{II} ^b	—	+0.77 V	+0.88 V (irr)
Cu ^{II} /Cu ^I ^c	—	-0.99 V	-0.95 V (irr.)
L _{Ru} /L _{Ru} ⁺ ^c	-1.77 V -1.98 V -2.35 V	—	-1.78 V -1.92 V -2.39 V

^aHalf-wave potentials E_{1/2} determined as (E_{pa} + E_{pc})/2 and reported versus Fc⁺⁰

^bMeasured on a Pt working electrode.

^cMeasured on a glassy carbon working electrode.